Journal of the American Ceramic Society,Volume 96, Issue 6, June 2013 pp. 1852–1856
DOI:10.1111/jace.12269

High tunability in (111)-oriented relaxor $Pb_{0.8}Ba_{0.2}ZrO_3$ thin film with antiferroelectric and ferroelectric two-phase coexistence

Biaolin Peng[1, 2], Huiqing Fan[1,*], Qi Zhang[2,*]

[1] State Key Laboratory of Solidification Processing, School of Materials Science and Engineering, Northwestern Polytechnical University, Xi'an 710072, China

[2] Department of Manufacturing and Materials, Cranfield University, Cranfield, Bedfordshire, MK43 0AL, United Kingdom

$Pb_{0.8}Ba_{0.2}ZrO_3$ (PBZ) thin film with a thickness of about 320 nm was fabricated on Pt(111)/TiO_x/SiO_2/Si substrate by a sol-gel method. The analysis results of XRD, SEM and dielectric propertities revealed that this thin film is a (111)-oriented nano-scaled antiferroelectric and ferroelectric two-phase coexisted relaxor. Calculations of dielectric tunability (η) and figure-of-merit (*FOM*) at room temperature display a maximum value of 75% at E = 560 kV/cm and ~ 236, respectively. High temperature stability (η > 75% and *FOM* > 230 at 560 kV/cm in the range from 300 K to 380 K) and high breakdown dielectric strength (leakage current < 1 nA at 598 kV/cm) make the PBZ thin film to be an attractive material for applications of tunable devices.

* E-mail: hqfan3@163.com, Tel:+44(0) 1234 750111, +44(0) 1234 751346
* E-mail: q.zhang@cranfield.ac.uk, Tel: +86-29-88494463, Fax: +86-29-88492642

I. Introduction

Dielectric tunable materials have recently received renewal attention due to the potential applications in filters, phase shifters, wireless communications, etc.[1-23] These applications demand dielectric materials possessing not only high dielectric tunability, but also low dielectric loss, high figure-of-merit and high temperature stability.[1-23] To accomplish these requirements, most research efforts in this area are focused on investigating titanium-containing perovskite ferroelectric materials such as $(Ba,Sr)TiO_3$ (BST),[15] $Ba(Zr,Ti)O_3$ (BZT),[16] $(Ba,Sn)TiO_3$,[22] and $(Pb,Sr)TiO_3$ (PST),[9] $Pb(Zr,Ti)O_3$[23], $(Pb,Ca)TiO_3$,[7] etc. Due to the oxidation state of titanium being easily reduced from Ti^{4+} to Ti^{3+},[24-29] the dielectric tunable properties of these titanium-containing ferroelectrics usually undergo degradation (dielectric loss increasing and figure-of-merit decreasing) at high temperature.

Many efforts have been made to improve the temperature stability of these dielectric tunable materials, such as doping with various oxides (MgO, Al_2O_3, ZrO_2, etc.) and elements (Mn^{2+}, Mn^{3+}, Fe^{2+}, Fe^{3+}, Co^{2+}, Co^{3+}, Ni^{2+}, etc.).[30-39] For thin films, in addition to the above-mentioned methods, many strategies, such as post thermal annealing, uses of buffer layers and/or oriented single-crystal substrates, and compositional gradation,[40-45] have been adopted to reduce the dielectric loss, modify the dielectric constants and improve the temperature stability. Additionally, the temperature stability can also be improved by making the materials behave as a relaxor with the diffuse phase transition[46] represented by the wide dielectric peak and frequency dependence.

In order to keep the reliabilities of tunable devices during the operations, traditional approaches, such as hermetic and robust packing,[47] were used to address the temperature instability issue of tunable devices based on a single composition of ferroelectric material. Robust packaging serves to protect tunable devices from harsh environmental conditions. This hermetic or robust packaging would add significant cost, size and weight to devices. Another approach is to use curve fitting (or look-up table).[47] Curve fitting approach uses the formulation of a temperature dependent mathematical expression to describe the drift of each tunable unit. A microprocessor inputs the ambient temperature data obtained by a thermocouple mounted on the printed circuit board in this mathematical expression to calculate tuning voltages, so that a stable tuning magnitude can be maintained. Obviously, these methods are too complex, time consuming and inaccurate.

In contrast to the engineering approaches, optimizing the response of materials to temperature variation is more convenient and effective. Adoption of double-phase, multi-phase or compositionally graded phase structures[47,48] may be a useful approach to design the material and thus realize the device temperature stability. In this work, a (111)-oriented nano-scaled antiferroelectric and ferroelectric two-phase coexisted relaxor $Pb_{0.8}Ba_{0.2}ZrO_3$ thin film was fabricated by a sol-gel method, and high temperature stability ($\eta > 75\%$ and FOM > 230 at 560 kV/cm in the range from 300 K to 380 K) was achieved, making this thin film comparable with those titanium-containing ferroelectric materials.

II. Experimental procedure

$Pb_{80}Ba_{20}ZrO_3$ (PBZ) thin film was fabricated by a sol-gel method. $Pb(OAc)_2 \cdot 3H_2O$ and $Ba(OAc)_2$ were dissolved in glacial acetic and deionized water. In order to compensate the Pb loss during sintering, 20% excess Pb was added. Separately, acetylacetone was added to a mixture of $Zr(O^nPr)_4$ and 2-methoxyethanol and the resulting solution was stirred for 30 min at room temperature. The Pb/Ba and Zr solutions were then mixed and stirred for 2 h at room temperature. The final concentration of the synthesized PBZ sol was 0.3 M. After aging the sol for 24 h, the PBZ sol was passed through a 0.2 μm filter and spun onto $Pt(111)/TiO_x/SiO_2/Si(100)$ substrates at 4000 rpm for 30 s. The substrates were rinsed with acetone and 1-propanol before use. Each layer was pyrolized at 350 °C for 3 min and then heated at 550 °C for 3 min on hotplates, and finally annealed at 800 °C for 3 min in a tube furnace in air. The above-mentioned procedure was repeated several times to obtain the desired thickness. Cr/Au top electrodes of 150 μm diameter were evaporated through a patterned photoresist mask.

The structure of the PBZ film was monitored by X-ray diffraction (XRD; Bruker-AXS D5005, Siemens, Munich, Germany) on a diffractometer, using Cu Kα radiation (λ=1.5406Å). The cross-sectional and surface morphologies of the film were examined by scanning electron microscope (SEM; FEI XL30 SFEG, Philips, Edihoven, The Netherlands). Dielectric permittivity measurements were carried out using an impedance analyzer (Wayne-Kerr Electronics, UK) at V = 100 mV. Electric field dependences of polarization hysteresis (*P*-*E*) loop and leakage current (*I*(*t*)) were obtained by means of a ferroelectric tester (RT66A, Radiant Technologies Inc.,

Albuquerque, NM, USA). The temperature of the sample was controlled via feedback from a thermocouple, accurate to 0.1 °C, in contact with the sample.

III. Results and discussions

Fig.1(a) shows the cross-sectional morphology of PBZ thin film, where uniform thickness (about 320 nm), and clearly visible layers were observed. XRD result (Fig.1(b)) further indicated that PBZ thin film was well crystallized into the pure perovskite phase with a higher intensity (111) orientation. Superlattice reflections with indices (130)/(112) and (014) indicate the existence of orthorhombic antiferroelectric phase[49] in the PBZ thin film. Refined lattice parameters for the orthorhombic antiferroelectric (O_{AFE}) phase are determined to be a_O = 5.83009 Å, b_O = 11.71391 Å and c_O = 8.31277 Å by using the software JADE. In addition to the O_{AFE} phase, a rhombohedral ferroelectric (R_{FE}) phase with lattice parameters a_R = 4.12483 Å and α_R = 90.9463 ° can also be detected. The SEM surface image (inset in Fig.1(b)) also revealed that the microstructure of PBZ thin film was uniform, homogeneous, and crack free, with average grain size of 20 nm.

To further study the morphology and microstructure of PBZ thin film in details, the TEM characterization was carried out. Numerous dispersed nanocrystals corresponding to those subgrains in the SEM were observed again in the TEM bright field image (Fig.1(c)). In the inside of some nanocrystals, lamellar nanodomains with about 2 nm wide (see the red dot circles) and lamellar nanodomains with about 1 nm wide (see the blue solid circles) are clearly visible. The latter can be attributed to the antiferroelectric domains with 1 nm wide close to its cell parameters, which is

consistent with the report by Viehland[50] in PZT. Inset of Fig. 1 (c) shows the selected area electron diffraction (SAED) pattern of PBZ thin film. For simplicity, the lattice indices for SAED were labeled as the pseudo cubic structure rather than the orthorhombic or rhombohedral structure. Circular rings correspond to the (111), (220), and (311) plane reflections (from inside to outside), respectively. The discontinuity of diffraction rings indirectly revealed the nanocrystalline characteristics of PBZ thin film.[51] It is well known that the polarization vector for the R_{FE} phase is <111>,[52] and the rotation between neighboring domains depends on the cell angle α. For PZT,[52] the rhombohedral angle α is 91°, and the possible types of domain can be calculated as 109°, 71°, and 180°. The orientation of permissible uncharged walls is {110} for 109°, {001} for 71° and the plane parellel to the polarization vector is 180° domain. According to the refined α value (90.9463°) of the R_{FE} phase and the feature of the SAED pattern of PBZ thin film, lamellar nanodomains with about 2 nm wide probably is due to the exisitence of 180° ferroelectric domains, which need to be further confirmed by the piezoresponse force microscopy (PFM).

Temperature dependences of dielectric permittivity (ε) and dielectric loss (tan δ) at 100 Hz, 1kHz, 10kHz and 100 kHz are shown in Fig.2(a). Typical ferroelectric relaxor character can be observed around the dielectric permittivity peak, in contrast, the same character cannot be detected in $Pb_{(1-x)}Ba_xZrO_3$ bulk ceramics with Ba^{2+} substitution at $x < 0.3$.[53] This difference can be attributed to the mismatch effect between the film and substrate and the smaller grain size. [54-56] Although the dielectric permittivity ($\varepsilon_m \sim 1650$ at 100 Hz) is higher compared with those found in PZT-based

compositions, it is rather lower than that obtained in corresponding sintered bulk PBZ ceramics with the same composition (ε_m ~ 12000),[53,57] which may most probably be due to the limited film thickness. Likewise, the maximum dielectric permittivity is observed at 433 K (T_m at 100 Hz), rather than at 425 K reported in PBZ bulk material.[53,57] The antiferroelectric to ferroelectric (AFE-FE) phase transition (see the red arrow) can be detected at 354 K, which can also be observed on the *P-T* (polarization vs temperature) curve plotted from the *P-E* (polarization vs electric field) loops at 10 kHz and 156 kV/cm, as shown in the inset of Fig.2 (a).

To further describe the dielectric relaxor behavior of PBZ thin film at $T > T_m$, the well-known empirical Lorentz-type relation was employed.[58-61]

$$\varepsilon_A / \varepsilon = 1 + (T - T_A)^2 / 2\delta_A^2 \quad (1)$$

where T_A ($T_A \neq T_m$) and ε_A are the temperature of the dielectric permittivity peak and the extrapolated value of ε at $T = T_A$, respectively. The parameter δ_A is almost temperature and frequency independent, reflecting the relaxor diffuseness of the dielectric peak. The greater the relaxor dispersion is, the bigger δ_A is. The colored solid lines in Fig.2(a) exhibit the best results of Lorentz fitting using Eq.(1). It was found that the Eq.(1) can describe the high temperature ($T > T_m$) dielectric permittivity quite well both at the high temperature range of $T > T_{AFE-FE}$ (the temperature of antiferroelectric to ferroelectric phase transition). Accordingly, the Lorentz fitting parameters δ_A for 100 Hz, 1 kHz, 10 kHz and 100 kHz are 100.69, 98.68, 97.73 and 97.62, respectively, indicating that the degree of relaxor dispersion decreases slightly with the increasing of frequency. Meanwhile, the δ_A of PBZ thin

film is close to that (103.6) of the prototypical relaxor $Pb(Mg_{1/3}Nb_{2/3})O_3$ (PMN) ceramics,[61] indicating that the large relaxation of the dielectric permittivity and typical relaxor behavior in the PBZ film. Furthermore, it can be clearly seen that the gap between the extrapolated value of Lorentz fitting and the experimental data increases gradually with the decrease of temperature from the T_{AFE-FE} to T_{room}, further revealing the coexistence of antiferroelectric and ferroelectric phases in PBZ thin film at room temperature.

Dc bias electric field dependences of dielectric permittivity ($\varepsilon(E)$) and dielectric loss (tan $\delta(E)$) at 10 kHz at room temperature are shown in Fig.2(b). Both $\varepsilon(E)$ and tan $\delta(E)$ exhibit butterfly-shaped curves, indicating a nonlinear electric field dependence. Negligible electrical hysteresis can be observed during the polarizing and depolarizing. Electric field induced AFE-FE (polarizing) or FE-AFE (depolarizing) phase transition occurs at about 75 kV/cm, which is revealed more clearly in the double *P-E* loop (see the inset of Fig.2(b)). Moreover, no degradation (dielectric loss increasing) undergoes even under a large external electric field (> 500 kV/cm) except in the process of AFE-FE or FE-AFE phase transition, in contrast, a terrible degradation usually caused by the reduction of Ti^{4+} to Ti^{3+} takes place in those of titanium-containing dielectric materials, which cannot be acceptable for the application of tunable devices.

Dielectric tunability (η) and Figure-of-merit (*FOM*) can be defined,[2] respectively, as follows:

$$\eta(\%) = (\varepsilon(0) - \varepsilon(E))/\varepsilon(0) \times 100 \quad (2)$$

$$FOM = \eta/\tan\delta \quad (3)$$

where $\varepsilon(0)$ and $\varepsilon(E)$ represent the dielectric permittivity at zero and a certain electric field, respectively. Fig. 3(a) illustrates the dielectric tunability ($\eta(E)$) and Figure-of-merit ($FOM(E)$) dependences of the dc bias electric field at 10 kHz at room temperature. It was found that the tunability increases with E and a 75% tunability are achieved at E = 560 kV/cm in both polarizing and depolarizing branches. Similar to tunability, FOM also increases with E and a maximum value of 236 is obtained, indicating that the PBZ thin film can be a very promising material for dielectric tunable device applications.

In the case of $\varepsilon >> 1$, the $\varepsilon(E)$ for perovskite-structure ferroelectric materials could be interpreted by the phenomenological theory proposed by Johnson, and is expressed as[62]:

$$\varepsilon(E) = \varepsilon(0)/\{1 + \varepsilon_0 \varepsilon(0)^3 \alpha_{(T)} E^2]\}^{1/3} \quad (4)$$

where ε_0 is the vacuum dielectric permittivity, $\alpha_{(T)}$ the temperature-dependent constant which provides information on the degree of enharmonic contributions of the polarization to the free energy. Combined with Eq.(2) and Eq.(4), a linear expression between dielectric tunability and dc bias electric field square (E^2) can be derived:

$$(1-\eta)^{-3} = 1 + [\varepsilon_0 \varepsilon(0)^3 \alpha_{(T)}] E^2 \quad (5)$$

The inset of Fig.3(a) shows the E^2 dependence of $(1-\eta)^{-3}$. It can be found that the experimental data are in a good agreement with Eq. (5) when E > 200 kV/cm (R-square > 99.9%), indicating that the dielectric tunable performance is mainly ascribed to the intrinsic lattice phonon polarization[11, 63]. Meanwhile, we found that the experimental data largely deviated from Eq.(5) when E < 200kV/cm (R-square <

80%), indicating that the re-orientation[63] of the nanopolar clusters[64] (in ferroelectric phase) and (or) the nanononpolar clusters (in antiferroelectric phase) plays an important role in the high dielectric tunability property (η is about 50% at 200 kV/cm) of PBZ thin film, in addition to the intrinsic lattice phonon polarization.

For a competent dielectric tunable material, not only high value of tunability and high Figure-of-merit are required, but also high temperature stability is necessary. Fig3.(b) presents the temperature dependences of the tunability and Figure-of-merit at E = 560 kV/cm and 10 kHz. With the increase of the temperature, the tunability first increases and reaches a maximum (about 84%) at 430 K, close to the T_m in Fig. 2(a), and then decreases. Different to the tunability, the maximum *FOM* (about 268) was observed at 345 K, close to the $T_{\text{AFE-FE}}$ (see Fig.2(a)), which can be ascribed to the smaller dielectric loss at $T_{\text{AFE-FE}}$. These results indicate the high temperature stability of tunable property of PBZ thin film, and are desired for the application of tunable devices, because of the *FOM* and tunability for dielectrics used in their paraelectric state usually tending to be deteriorated during the operations, caused by a rise of temperature, especially for those titanium-containing dielectric materials.

Moreover, a low leakage current (I(t)) during the operation is also another important qualification for thin films. For PBZ thin film, the measurement of leakage currents (see the inset of Fig.3 (b)) was carried out at 598 kV/cm at room temperature. It is found that no breakdown occurs (breakdown at 688 kV/cm) after repetitive testing even in the observed transients persisting up to 1000 ms, and the maximum value of leakage currents is below 1 nA, indicating the high dielectric strength of PBZ

thin film.

IV. Conclusions

(111)-oriented nano-scaled antiferroelectric and ferroelectric phases coexisted relaxor $Pb_{0.8}Ba_{0.2}ZrO_3$ thin film was successfully prepared by a sol-gel method. The dielectric relaxor dispersion character of this film can be well described by the Lorentz-type relation. The high dielectric tunability (η ~ 75%), figure-of-merit (FOM ~ 236), temperature stability (η > 75% and FOM > 230 at 560 kV/cm in the range from 300 K to 380 K) and high dielectric strength (leakage current < 1 nA at 598 kV/cm) make it a promising material for applications of tunable devices. In addition to the contribution from intrinsic lattice phonon polarization, the re-orientation of nanoclusters in ferroelectric and antiferroelectric phases plays a crucial role in the high dielectric tunability.

Acknowledgements

Peng would like to thank National Natural Science Foundation (51172187), the SPDRF (20116102130002) and 111 Program (B08040) of MOE, and the Xi'an Science and Technology Foundation (CX1261-2, CX1261-3, XA-AM-201003) of China for personel financial support for working in Cranfield.

References

[1] Jinfei Wang, Tongqing Yang, Kun Wei, Gang Li, and Shengchen Chen, "Bi-Tunable Dielectric Constant of Antiferroelectric PZT Ceramics Under DC Electric Field," J. Am. Ceram. Soc., 95 [5] 1483-1485 (2012).

[2] T. M. Correia and Q. Zhang, "High tunable dielectric response of $Pb_{0.87}Ba_{0.1}La_{0.02}(Zr_{0.6}Sn_{0.33}Ti_{0.07})O_3$ thin film," J. Appl. Phys., 108 [4] 044107 3pp (2010).

[3] F. Zimmermann, M. Voigts, W. Menesklou, and E. Ivers-Tiffée, "$Ba_{0.6}Sr_{0.4}TiO_3$ and $BaZr_{0.3}Ti_{0.7}O_3$ thick films as tunable microwave dielectrics," J. Eur. Ceram. Soc., 24 [6] 1729-1733 (2004).

[4] Yaoyang Liu, Xiaomei Lu, Yaming Jin, Song Peng, Fengzhen Huang, Yi Kan, Tingting Xu, Kangli Min, and Jinsong Zhu, "Tunable electric properties of $PbZrO_3$ films related to the coexistence of ferroelectricity and antiferroelectricity at room temperature," Appl. Phys. Lett., 100 [21] 212902 4pp (2012).

[5] K. Khamchane, A. Vorobiev, T. Claeson, and S. Gevorgian, "$Ba_{0.25}Sr_{0.75}TiO_3$ thin-film varactors on $SrRuO_3$ bottom electrode," J. Appl. Phys., 99 [3] 034103 8pp (2006).

[6] Biaolin Peng, Huiqing Fan, and Qi Zhang, "The Contribution of the Extrinsic Polarizations to the Dielectric Tunability of $Pb(Mg_{1/3}Nb_{2/3})_{1-x}Ti_xO_3$ Relaxor Ferroelectrics" J. Am. Ceram. Soc., 95 [5] 1651-1655 (2012).

[7] M. L. Calzada, I. Bretos, R. Jime´nez, J. Ricote, and J. Mendiola, "Chemical Solution Deposition of $(Pb_{1-x}Ca_x)TiO_3$ Thin Films with x ~ 0.5 as New Dielectrics for

Tunable Components and Dynamic Random Access Memories," J. Am. Ceram. Soc., 88 [12] 3388-3396 (2005).

[8] Y. C. Lee, T. P. Hong, and K. H. Ko, "Low-voltage and high-tunability interdigital capacitors employing lead zinc niobate thin films," Appl. Phys. Lett., 90 [18] 182908 6pp (2007).

[9] Jiwei Zhai and Xi Yao, "Effect of Orientation on the Ferroelectric Behavior of (Pb,Sr)TiO_3 Thin Films," J. Am. Ceram. Soc., 89 [1] 354-357 (2006).

[10] C. Ang, A. S. Bhalla, and L. E. Cross, "Dielectric behavior of paraelectric $KTaO_3$, $CaTiO_3$, and $(Ln_{1/2}Na_{1/2})TiO_3$ under a dc electric field," Phys. Rev. B, 64 [18] 184104 6pp (2001).

[11] Biaolin Peng, Huiqing Fan, Qiang Li, and Qi Zhang, "High dielectric non-linear properties of the $Pb[(Mg_{1/3}Nb_{2/3})_{0.8}(Sc_{1/2}Nb_{1/2})_{0.2}]O_3$ ceramics," Mat. Res. Bull., 47 [8] 2051-2055 (2012).

[12] Lin-Jung Wu and Jenn-Ming Wu, "Improved dielectric properties of Al_2O_3-doped $Pb_{0.6}Ba_{0.4}ZrO_3$ thin films for tunable microwave applications," Appl. Phys. Lett., 91 [13] 132909 3pp (2007).

[13] L. P. Curecheriu, A. Ianculescu, and L. Mitoseriu, "Tunability properties in the paraelectric state of the $Pb(Mg_{1/3}Nb_{2/3})O_3$ ceramics," J. Eur. Ceram. Soc., 30 [2] 599-603 (2010).

[14] Chen Ang, Zhi Yu, and Zhi Jing, "Impurity-induced ferroelectric relaxor behavior in quantum paraelectric $SrTiO_3$ and ferroelectric $BaTiO_3$," Phys. Rev. B, 61 [2] 957-961 (2000).

[15] Lihui Yang, Genshui Wang, Xianlin Dong, and Denis Re´miens, "Improved Dielectric Properties of $Bi_{1.5}Zn_{1.0}Nb_{1.5}O_7$/(111)-Oriented $Ba_{0.6}Sr_{0.4}TiO_3$ Bilayered Films for Tunable Microwave Applications," J. Am. Ceram. Soc., 93 [5] 1215-1217 (2010).

[16] Xiujian Chou, Jiwei Zhai, and Xi Yao, "Relaxor Behavior and Dielectric Properties of $MgTiO_3$-Doped $BaZr_{0.35}Ti_{0.65}O_3$ Composite Ceramics for Tunable Applications," J. Am. Ceram. Soc., 90 [9] 2799-2801 (2007).

[17] X. G. Tang, K.-H. Chew, J. Wang, and H. L. W. Chan, "Dielectric tunability of $(Ba_{0.90}Ca_{0.10})(Ti_{0.75}Zr_{0.25})O_3$ ceramics," Appl. Phys. Lett., 85 [6] 991 3pp (2004).

[18] Y. Somiya, A. S. Bhalla, and L. E. Cross, "Stdudy of $(Sr,Pb)TiO_3$ ceramics on dielectric and physical properties," Int. J. Inorg. Mater., 3 [7] 709-714 (2001).

[19] K.F. Astafiev, V.O. Sherman, A.K. Tagantsev, and N. Setter, "Can the addition of a dielectric improve the figure of merit of a tunable material," J. Eur. Ceram. Soc., 23 [14] 2381-2386 (2003).

[20] J. Lindner, F. Weiss, J.-P Sénateur, V. Galindo, W. Haessler, M. Weihnacht, J. Santiso, and A. Figueras, "Growth of $YBa_2Cu_3O_{7-x}/Ba_xSr_{1-x}TiO_3/LaAlO_3$ heterostructures by injection MOCVD for microwave applications," J. Eur. Ceram. Soc., 19 [6-7] 1435-1437 (1999).

[21] L. P. Curecheriu, L. Mitoseriu, and A. Lanculescu, "Tunability properties of the $Pb(Mg_{1/3}Nb_{2/3}O_3)$ relaxors and theoretical description," J. Alloys and Compd., 485 [1-2] 1-5 (2009).

[22] S. G. Lu and Z. K. Xu, "Tunability and permittivity-temperature characteristics

of highly (100) oriented compositionally graded $(Ba_{0.7}Sr_{0.3})(Sn_xTi_{1-x})O_3$ thin films grown by pulse-laser deposition," Appl. Phys. Lett., 89 [15] 152907 3pp (2006),

[23] Jiagang Wu, Dingquan Xiao, Yuanyu Wang, Jianguo Zhu, Jiliang Zhu, and Ruishi Xie, "High Tunability of Highly (100)-Oriented Lead Zirconate Titanium Thin Films," J. Am. Ceram. Soc., 91 [11] 3786-3788 (2008).

[24] Yuanyuan Zhang, Genshui Wang, Ying Chen, Fei Cao, Lihui Yang, and Xianlin Dong, "Effect of Donor, Acceptor, and Donor-Acceptor Codoping on the Electrical Properties of $Ba_{0.6}Sr_{0.4}TiO_3$ Thin Films for Tunable Device Applications," J. Am. Ceram. Soc., 92 [11] 2759-2761 (2009).

[25] G. Lu, A. Linsebigler, and J. T. Yates, "Ti^{3+} Defect Sites on TiO_2 (110)-Production and Chemical Detection of Active-sites," J. Phys. Chem., 98 [45] 11733 (1994).

[26] Xihong Hao, Jiwei Zhai, Huiping Ren, Xiwen Song, and Jichun Yang, "Fabrication and Tunable Dielectric Properties of Magnesium-Doped Lead Barium Zirconate Thin Films," J. Am. Ceram. Soc., 93 [3] 646-649 (2010).

[27] Ya-Ling Kuo and Jenn-Ming Wu, ''Tunable Dielectric Properties of Lead Barium Zirconate Niobate Films,'' Appl. Phys. Lett., 89 [13] 132911, 3pp (2006).

[28] Xihong Hao, Jiwei Zhai, and Xi Yao, "Dielectric Tunable Properties Relaxor Behavior of $(Pb_{0.5}Ba_{0.5})ZrO_3$ Thin Films," J. Am. Ceram. Soc., 91 [12] 4112-4114 (2008).

[29] Mei-Hai Wu and Jenn-Ming Wu, "Lead barium zirconate perovskite films for

electrically tunable applications," Appl. Phys. Lett., 86 [2] 022909 3pp (2005).

[30] M. Jain, S.B. Majumder, R.S. Katiyar, F.A. Miranda, and F.W. Van Keuls, "Improvement in electrical characteristics of graded manganese doped barium strontium titanate thin films," Appl. Phys. Lett., 82 [12] 1911 3pp (2003).

[31] M.W. Cole, C. Hubbard, E. Ngo, M. Ervin, M. Wood, and R.G. Geyer, "Structure–property relationships in pure and acceptor-doped $Ba_{1-x}Sr_xTiO_3$ thin films for tunable microwave device applications," J. Appl. Phys., 92 [1] 475 9pp (2002).

[32] P.C. Joshi and M.W. Cole, "Mg-doped $Ba_{0.6}Sr_{0.4}TiO_3$ thin films for tunable microwave applications," Appl. Phys. Lett., 77 [2] 289 3pp (2000).

[33] S.Y. Wang, B.L. Cheng, Can Wang, S.Y. Dai, H.B. Lu, Y.L. Zhou, Z.H. Chen, and G.Z. Yang, "Reduction of leakage current by Co doping in $Pt/Ba_{0.5}Sr_{0.5}TiO_3/Nb\text{-}SrTiO_3$ capacitor," Appl. Phys. Lett., 84 [20] 4116 3pp (2004).

[34] M. W. Cole, P. C. Joshi, and M. H. Ervin, "La doped $Ba_{1-x}Sr_xTiO_3$ thin films for tunable device applications," J. Appl. Phys., 89 [11] 6336 5pp (2001).

[35] K. B. Chong, L. B. Kong, Linfeng Chen, L. Yan, C. Y. Tan, T. Yang, C. K. Ong, and T. Osipowicz, "Improvement of dielectric loss tangent of Al_2O_3 doped $Ba_{0.5}Sr_{0.5}TiO_3$ thin films for tunable microwave devices," J. Appl. Phys., 95 [3] 1416 4pp (2004).

[36] Z. Yuan, Y. Lin, J. Weaver, X. Chen, C. L. Chen, G. Subramanyam, J. C. Jiang, and E. I. Meletis, ''Large Dielectric Tunability and Microwave Properties of Mn-Doped $(Ba,Sr)TiO_3$ Thin Films,'' Appl. Phys. Lett., 87 [15] 152901 3pp (2005).

[37] L. N. Gao, J. W. Zhai, and X. Yao, ''The Influence of Co Doping on the

Dielectric, Ferroelectric and Ferromagnetic Properties of $Ba_{0.70}Sr_{0.30}TiO_3$ Thin Films,'' Appl. Surf. Sci., 255 [8] 4521 5pp (2009).

[38] K. Imai, S. Takeno, and K. Nakamura, ''Effect of Fe Doping of Thin (Ba,Sr)TiO_3 Films on Increase in Dielectric Constant,'' Jpn. J. Appl. Phys., 41 [10] 6060 5pp (2002).

[39] W. Y. Park, C. S. Hwang, J. D. Baniecki, M. Ishii, K. Kurihara, and K. Yamanaka, ''Unusual Thickness Dependence of Permittivity and Elastic Strain in Sc Modified Epitaxial (Ba,Sr)TiO_3 Thin Films,'' Appl. Phys. Lett., 92 [10] 102902 3pp (2008).

[40] Young-Ah Jeon, Eun-Suck Choi, Tae-Suck Seo, and Soon-Gil Yoon, "Improvements in tunability of $(Ba_{0.5}Sr_{0.5})TiO_3$ thin films by use of metalorganic chemical vapor deposited (Ba,Sr)RuO_3 interfacial layers," Appl. Phys. Lett., 79 [7] 1012 3pp (2001).

[41] T. M. Shaw, Z. Suo, M. Huang, E. Liniger, R. B. Laibowitz, and J. D. Baniecki, "The effect of stress on the dielectric properties of barium strontium titanate thin films," Appl. Phys. Lett., 75 [14] 2129 3pp (1999).

[42] T. R. Taylor, P. J. Hansen, B. Acikel, N. Pervez, R. A. York, S. K. Streiffer, and J. S. Speck, "Impact of thermal strain on the dielectric constant of sputtered barium strontium titanate thin films," Appl. Phys. Lett., 80 [11] 1978 3pp (2002).

[43] Weicheng Zhu, Jinrong Cheng, Shengwen Yu, Jia Gong, and Zhongyan Meng, "Enhanced tunable properties of $Ba_{0.6}Sr_{0.4}TiO_3$ thin films grown on Pt/Ti/SiO_2/Si substrates using MgO buffer layers," Appl. Phys. Lett., 90 [3] 032907 3pp (2007).

[44] Z. Ying, P. Yun, D. Y. Wang, X. Y. Zhou, Z. T. Song, S. L. Feng, Y. Wang, and H. L. W. Chan, "Fine-grained $BaZr_{0.2}Ti_{0.8}O_3$ thin films for tunable device applications" J. Appl. Phys., 101 [8] 086101 3pp (2007).

[45] X. H. Zhu, J. Li, and D. N. Zheng "Frequency and temperature dependence of tunable dielectric properties of $Ba(Zr_{0.2}Ti_{0.8})O_3$ thin films grown on (001) MgO," Appl. Phys. Lett., 90 [14] 142913 3pp (2007).

[46] Yidong Xia, Cong Cai, Xiaoyuan Zhi, Bai Pan, Di Wu, Xiangkang Meng, and Zhiguo Liub, "Effects of the substitution of Pb for Ba in $(Ba,Sr)TiO_3$ films on the temperature stability of the tunable properties," Appl. Phys. Lett., 88 [18] 182909 3pp (2006).

[47] M. W. Cole, E. Ngo, S. Hirsch, J. D. Demaree, S. Zhong, and S. P. Alpay, "The fabrication and material properties of compositionally multilayered $Ba_{1-x}Sr_xTiO_3$ thin films for realization of temperature insensitive tunable phase shifter devices," J. Appl. Phys., 102 [3] 034104 11pp (2007).

[48] M. W. Cole, C. V. Weiss, E. Ngo, S. Hirsch, L. A. Coryell, and S. P. Alpay, "Microwave dielectric properties of graded barium strontium titanate films," Appl. Phys. Lett., 92 [18] 182906 3pp (2008).

[49] Bhadra P. Pokharel and Dhananjai Pandey, "High temperature x-ray diffraction studies on antiferroelectric and ferroelectric phase transitions in $(Pb_{1-x}Ba_x)ZrO_3$ (x = 0.05,0.10)," J. Appl. Phys., 90 [6] 2985 10pp (2001).

[50] Dwight Viehland, "Transmission electron microscopy study of high-Zr-content lead zirconate titanate," Phys. Rev. B, 52[2] 778-791 (1995).

[51] Satyendra Singh and S. B. Krupanidhi, "Perovskite phase transformation in $0.65Pb(Mg_{1/3}Nb_{2/3})O_3$-$0.35PbTiO_3$ nanoparticles derived by sol-gel," J. Appl. Phys., 111[2] 024314 5pp (2012).

[52] J. Ricote, R. W. Whatmore, and D. J. Barber, "Studies of the ferroelectric domain configuration and polarization of rhombohedral PZT ceramics," J. Phys.: Condens. Matter, 12[3] 323-337 (2000).

[53] Bhadra P. Pokharel and Dhananjai Pandey, "Dielectric studies of phase transitions in $(Pb_{1-x}Ba_x)ZrO_3$," J. Appl. Phys., 88 [9] 5364 10pp (2000).

[54] E. A. Eliseev and M. D. Glinchuk, "Static properties of relaxor ferroelectric thin films," J. Appl. Phys., 102 [10] 104110 6pp (2007).

[55] C. Ziebert, H. Schmitt, J. K. Krüger, A. Sternberg, and K.-H. Ehses, "Grain-size-induced relaxor properties in nanocrystalline perovskite films," Phys. Rev. B, 69 [21] 214106 10pp (2004).

[56] Margarita Correa, Ashok Kumar, and Ram S. Katiyar, "Strain-Induced Relaxor Behavior in $PbSc_{0.50}Nb_{0.25}Ta_{0.25}O_3$ Thin Films: A Comparison with Nanoceramics," J. Am. Ceram. Soc., 91 [6] 1788-1795 (2008).

[57] Bhadra P. Pokharel, Dhananjai Pandey, V. Siruguri, and S. K. Paranjpe, Appl. Phys. Lett., 74 [5] 756 3pp (1999).

[58] A. A. Bokov and Z.-G. Ye, "Phenomenological description of dielectric permittivity peak in relaxor ferroelectrics," Solid State Commun., 116 [2] 105-108 (2000).

[59] A. A. Bokov, Y.-H. Bing, W. Chen, Z.-G. Ye, S. A. Bogatina, I. P. Raevski, S. I. Raevskaya, and E. V. Sahkar, "Empirical scaling of the dielectric permittivity peak in relaxor ferroelectrics," Phys. Rev. B., 68 [5] 052102 4pp (2003).

[60] C. Lei, A. A. Bokov, and Z.-G. Ye, "Ferroelectric to relaxor crossover and dielectric phase diagram in the $BaTiO_3$-$BaSnO_3$ system," J. Appl. Phys., 101 [8] 084105 9pp (2007).

[61] Shanming Ke, Huiqing Fan, Haitao Huang, and H. L. W. Chan, "Lorentz-type relationship of the temperature dependent dielectric permittivity in ferroelectrics with diffuse phase transition," Appl. Phys. Lett., 93 [11] 112906 3pp (2008).

[62] K. M. Johnson, "Variation of Dielectric constant with Voltage in Ferroelectrics and Its Application to Parametric Device," J. Appl. Phys., 33 [9] 2826 6pp (1962).

[63] Chen Ang and Zhi Yu, "dc electric-field dependence of the dielectric constant in polar dielectrics: Multipolarization mechanism model," Phys. Rew. B, 69[17] 174109 8pp (2004).

[64] Desheng Fu, Hiroki Taniguchi, Mitsuru Itoh, Shin-ya Koshihara, N. Yamamoto, and Shigeo Mori, "Relaxor $Pb(Mg_{1/3}Nb_{2/3})O_3$: A Ferroelectric with Multiple Inhomogeneities," Phys. Rev. Lett., 103[20] 207601 4pp (2009).

Captions

Fig. 1. (a) SEM cross-sectional morphology of the PBZ thin film; (b) XRD patterns and SEM surface image (inset); (c) TEM image and SAED pattern (inset).

Fig. 2. (a) $\varepsilon(T)$ and tan $\delta(T)$ of PBZ thin film. The colored solid lines are the results of Lorenz fitting and the inset is $P(T)$ at 156 kV/cm; (b) $\varepsilon(E)$ and tan $\delta(E)$ at 10 kHz at room temperature, the inset is *P*-*E* loop.

Fig. 3. (a) $\eta(E)$ and $FOM(E)$ at 10 kHz at room temperature, the inset is the $(1-\eta)^{-3}$ vs $E^2/1000$; (b) $\eta(T)$ and $FOM(T)$ at 562 kV/cm in the range from 298 K to 478 K, the colored solid lines represent fourth order polynomial fits to experimental data and the inset is $I(t)$ at 598 kV/cm.

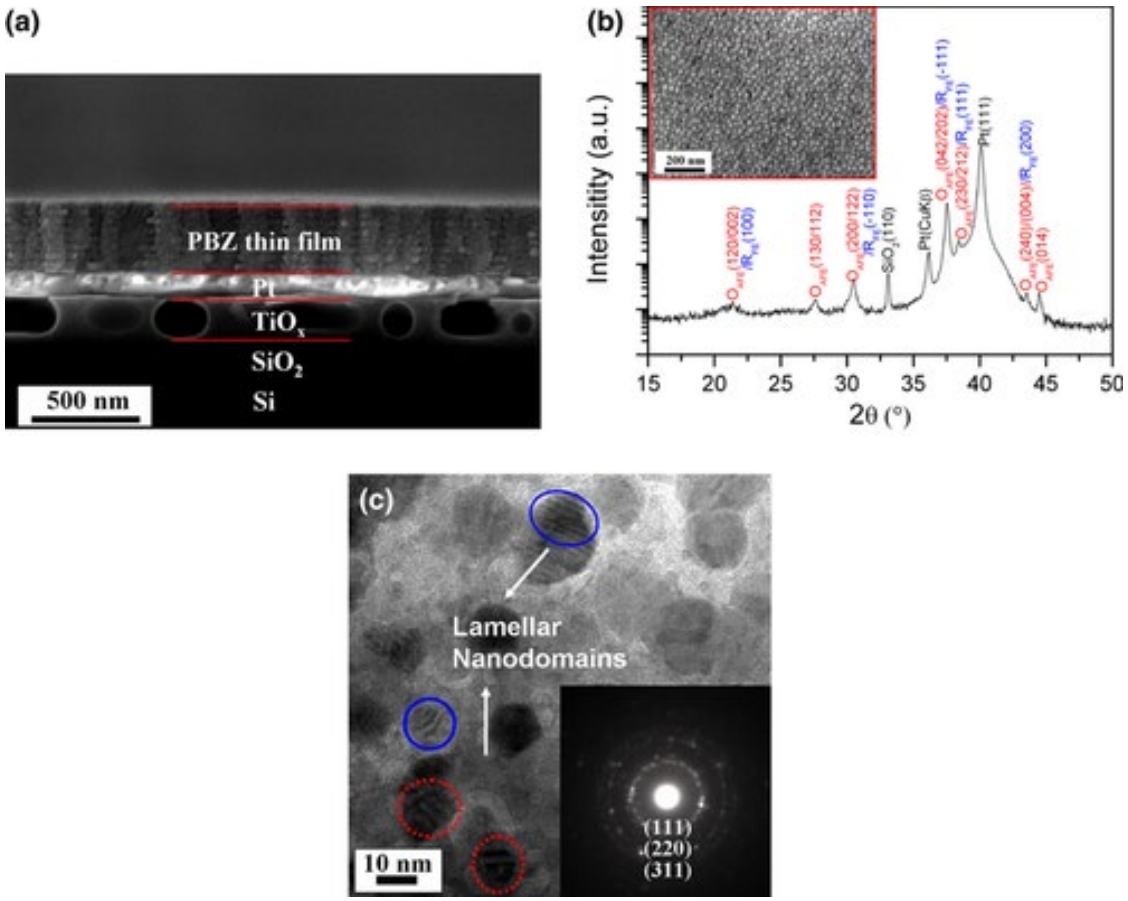

Figure 1
(a) SEM cross-sectional morphology of the PBZ thin film; (b) XRD patterns and SEM surface image (inset); (c) TEM image and SAED pattern (inset).

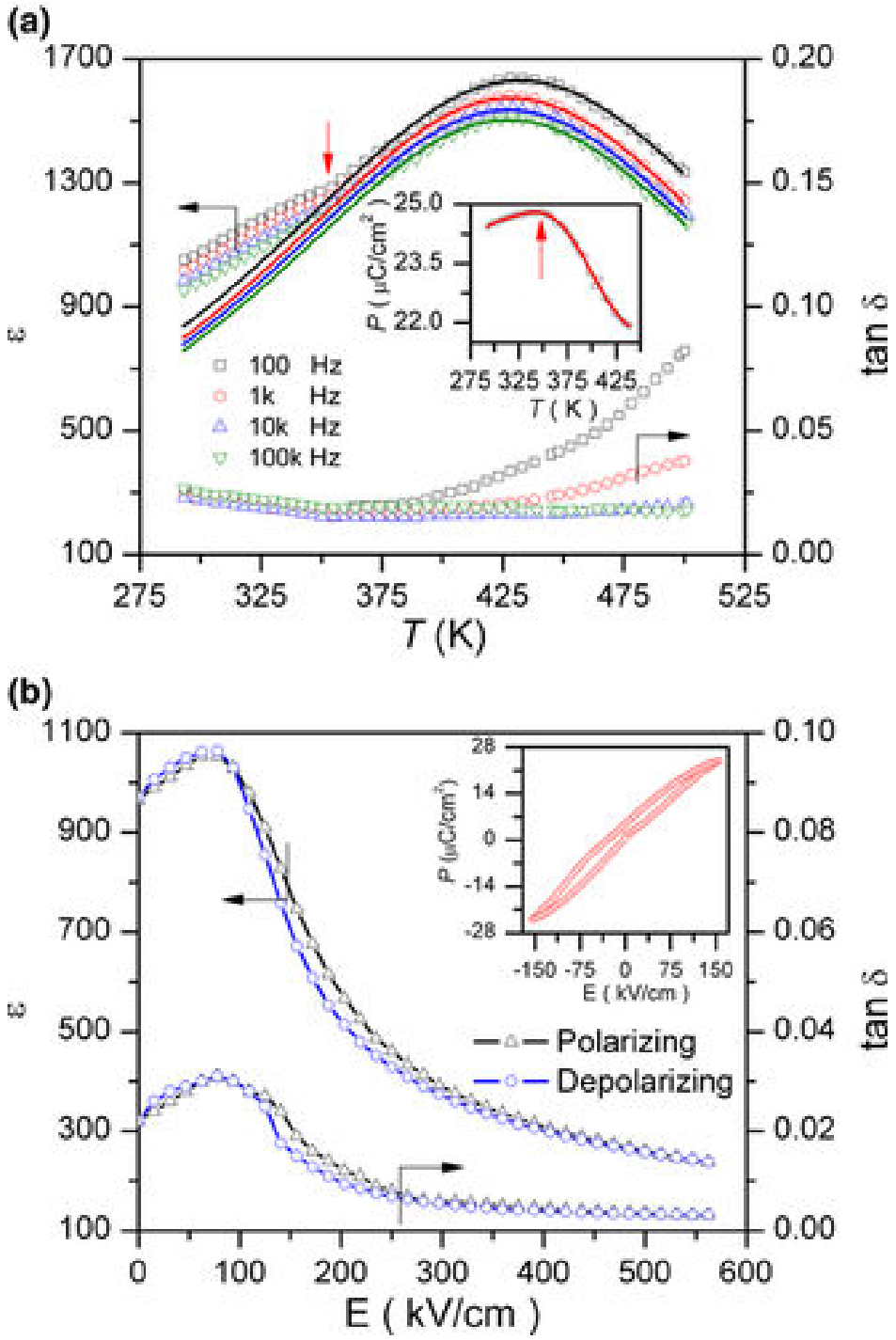

Figure 2
(a) ε(*T*) and tan δ(*T*) of PBZ thin film. The colored solid lines are the results of Lorenz fitting and the inset is *P*(*T*) at 156 kV/cm; (b) ε(*E*) and tan δ(*E*) at 10 kHz at room temperature, the inset is *P*–*E* loop.

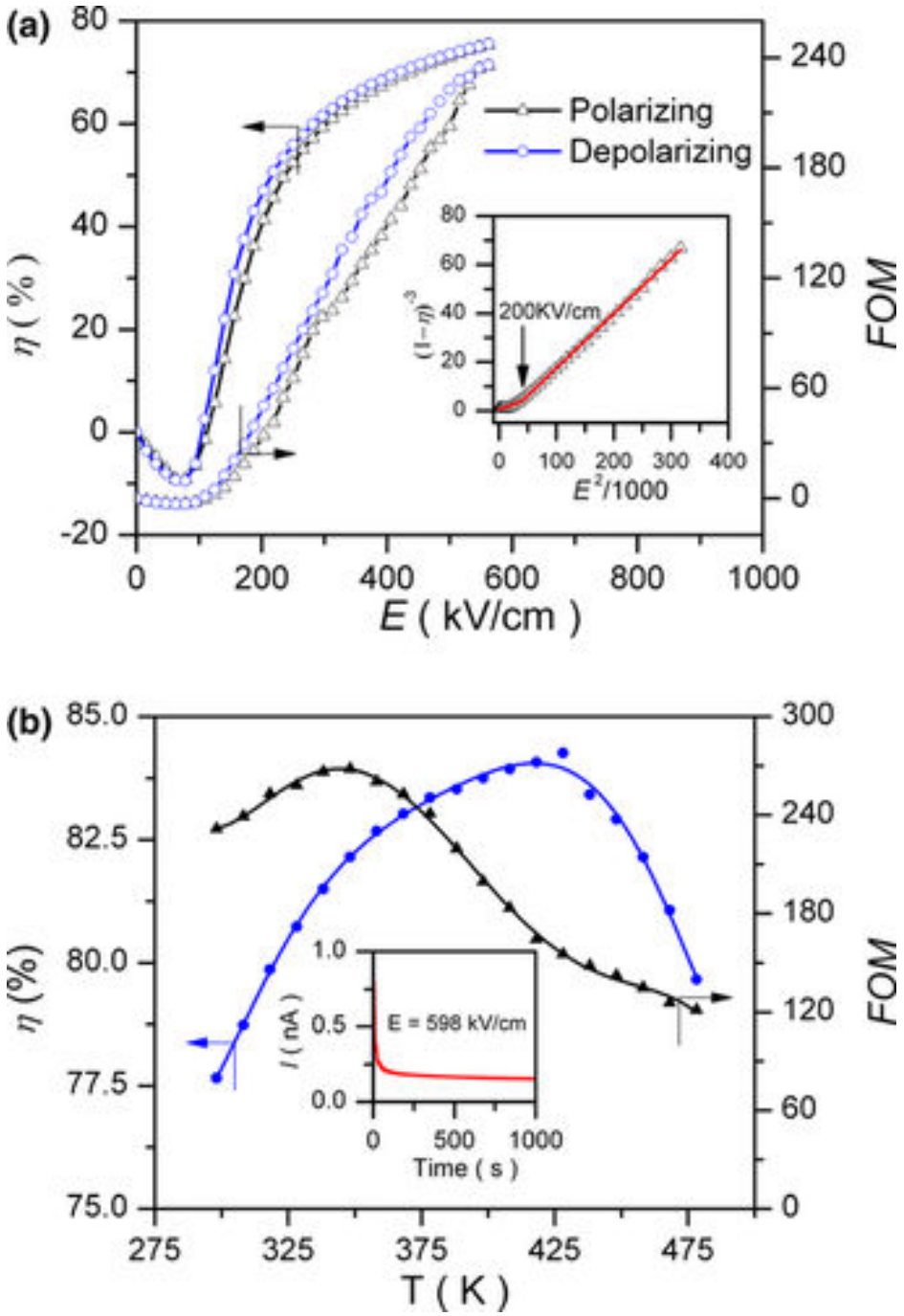

Figure 3
(a) η(*E*) and FOM (*E*) at 10 kHz at room temperature, the inset is the $(1-\eta)^{-3}$ versus $E^2/1000$; (b) η(*T*) and FOM(*T*) at 562 kV/cm in the range from 298 to 478 K, the colored solid lines represent fourth-order polynomial fits to experimental data and the inset is *I*(*t*) at 598 kV/cm.

2013-03-22

High tunability in (111)-oriented relaxor Pb0.8Ba0.2ZrO3 thin film with antiferroelectric and ferroelectric two-phase coexistence

Peng, Biaolin

Wiley

Peng B, Fan H, Zhang Q. (2013) High tunability in (111)-oriented relaxor Pb0.8Ba0.2ZrO3 thin film with antiferroelectric and ferroelectric two-phase coexistence. Journal of the American Ceramic Society, Volume 96, Issue 6, June 2013, pp. 1852-1856

https://doi.org/10.1111/jace.12269